1. Farkas,J.,Jármai,K.: **Minimum cost design and comparison of uniaxially compressed plates with welded flat, L- and trapezoidal stiffeners,** *52nd Annual Assembly of International Institute of Welding,* Lisboa, July 17-22, 1999, IIW-Doc. XV-1024-99, 12 p.

International Institute of Welding
Hungarian Delegation

Institut International de la Soudure
Délégation Hongroise

Minimum cost design and comparison of uniaxially compressed plates with welded flat, L- and trapezoidal stiffeners

Farkas,J. and Jármai, K.

University of Miskolc, Hungary

IIW-Doc. XV- 1024 –99 , XV-F-71-99

Lisboa, 1999

Abstract: The cost function to be minimized expresses the material and fabrication costs. Design constraints are as follows: global buckling of the uniaxially compressed longitudinally stiffened plate, local buckling of plate and stiffener elements, torsional buckling of open-section ribs, limitation of the thickness of cold-formed L- and trapezoidal stiffeners, limitation of the distortion caused by shrinkage of welds. The optimum dimensions and number of stiffeners are determined by a mathematical programming method. The cost comparisons show that, in the case of the treated illustrative numerical example, flat stiffeners give the cheapest solution, the cost of the plates with trapezoidal and L-stiffeners is 3.6% and 10% larger, respectively. The cost differences between the best and worst solutions are 6-11%, so the optimization results in significant cost savings.

Keywords: structural optimization, minimum cost design, welded structures, stiffened plates, buckling of compressed plates, distortion prevention

1. Introduction

Welded stiffened plates are widely used in various load-carrying structures, e.g. ships, bridges, bunkers, tank roofs, offshore structures, vehicles, etc. They are subject to various loadings, e.g. compression, bending, shear or combined load. The shape of plates can be square rectangular, circular, trapezoidal, etc. They can be stiffened in one or two directions with stiffeners of flat, L, trapezoidal or other shape.

From these structural versions we select here rectangular plates uniaxially compressed and stiffened in the direction of the compressive load. It should be mentioned that we have worked out minimum cost design procedure of square and rectangular orthogonally stiffened and cellular plates loaded in bending [1], uniaxially compressed rectangular plates with flat and L-stiffeners [2], welded bridge decks with open- and closed-section stiffeners [3,4].

It is well known that the instability phenomena are significantly affected by initial imperfections and residual welding stresses. For instance, it has been shown that a compression strut designed using the classical Euler method can be 30% unsafe [1]. Thus, these effects should be considered in all stability calculations.

In [2] we have used the design rules of API [5]. Mikami and Niwa [6,7] have recently developed a calculation method for orthogonally stiffened uniaxially compressed rectangular plates taking into account the initial imperfections and residual welding stresses. Their formulae are based on experimental results.

The aim of the present study is to apply the Mikami-Niwa method for the optimum design and comparison of uniaxially compressed plates stiffened with ribs of various shapes (Fig.1). In the minimum cost design the characteristics of the optimal structural version are sought which minimize the cost function and fulfil the design constraints. In recent years we have developed a cost function containing the material and fabrication costs [1,8] and we have included in the design constraints also the quality requirement, which prescribes the allowable deformation caused by residual welding distortions [9,10].

These two important aspects in the design of welded structures are included in the present study as well, to have a realistic basis for comparison. First the general formulae for the cost function and design constraints are treated, then the special calculation of flat, L- and trapezoidal stiffeners is described. A numerical example illustrates the differences among the structural versions.

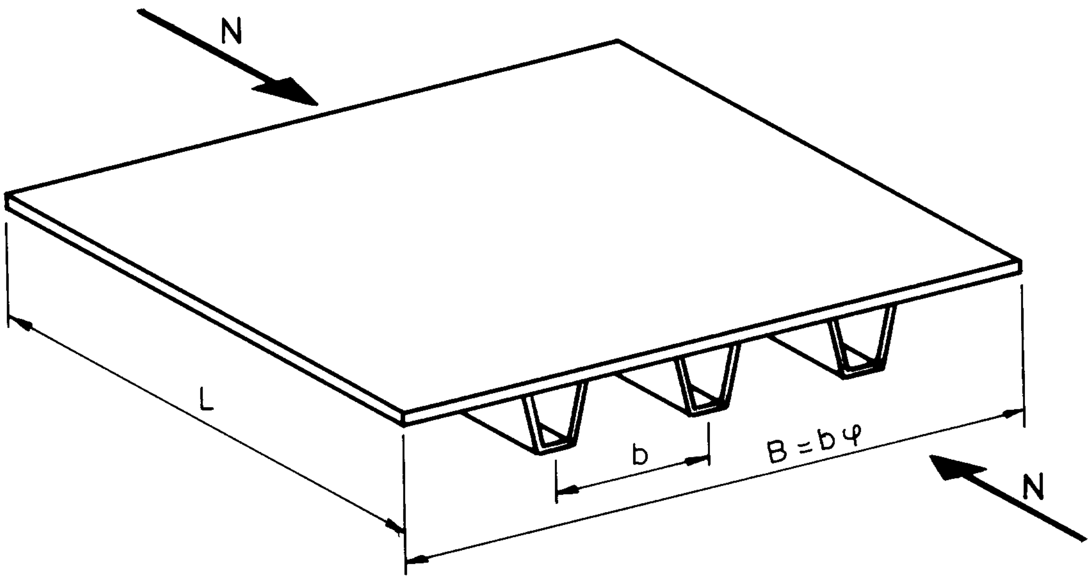

Fig.1. A uniaxially compressed longitudinally stiffened plate

2. Cost function

The objective function to be minimized is defined as the sum of material and fabrication costs

$$K = K_m + K_f = k_m \rho V + k_f \sum T_i \tag{1}$$

or in another form

$$\frac{K}{k_m} = \rho V + \frac{k_f}{k_m}\left(T_1 + T_2 + T_3\right) \tag{2}$$

where ρ is the material density, V is the volume of the structure, K_m and K_f as well as k_m and k_f are the material and fabrication costs as well as cost factors, respectively, T_i are the fabrication times as follows:

time for preparation, tacking and assembly

$$T_1 = \Theta_d \sqrt{\kappa \rho V} \tag{3}$$

where Θ_d is a difficulty factor expressing the complexity of the welded structure, κ is the number of structural parts to be assembled;

T_2 is time of welding, and T_3 is time of additional works such as changing of electrode, deslagging and chipping. $T_3 \approx 0.3 T_2$, thus,

$$T_2 + T_3 = 1.3 \sum C_{2i} a_{wi}^n L_{wi} \tag{4}$$

where L_{wi} is the length of welds, the values of $C_{2i} a_{wi}^n$ can be obtained from formulae or diagrams constructed using the COSTCOMP software [11,12], a_w is the weld dimension.

3. Design constraints

3.1 Global buckling of the stiffened plate

According to Mikami and Niwa the effect of initial imperfections and residual welding stresses is considered by defining buckling curves for a reduced slenderness

$$\lambda = \left(f_y / \sigma_{cr} \right)^{1/2} \tag{5}$$

where σ_{cr} is the classical critical buckling stress, which does not contain the above mentioned effects, f_y is the yield stress.

The classical critical buckling stress for a uniaxially compressed longitudinally stiffened plate (Fig.1) is

$$\sigma_{cr} = \frac{\pi^2 D}{hB^2}\left(\frac{1+\gamma_S}{\alpha_R^2} + 2 + \alpha_R^2 \right) \quad \text{for} \quad \alpha_R = L/B < \alpha_{R0} = \left(1+\gamma_S\right)^{1/4} \tag{6}$$

$$\sigma_{cr} = \frac{2\pi^2 D}{hB^2}\left[1 + \left(1+\gamma_S\right)^{1/2} \right] \quad \text{for} \quad \alpha_R \ge \alpha_{R0} \tag{7}$$

where, with $\nu = 0.3$

$$D = \frac{Et_F^3}{12\left(1-\nu^2\right)} = \frac{Et_F^3}{10.92} \tag{8}$$

$$h = t_F + \frac{A_S}{bt_F}\ ; \qquad b = \frac{B}{\varphi} \tag{9}$$

A_S is the cross-sectional area of a stiffener, $\varphi - 1$ is the number of stiffeners,

$$\gamma_S = \frac{EI_S}{bD} \tag{10}$$

I_S is the moment of inertia of a stiffener about the ξ axis (Fig.4).

Knowing the reduced slenderness (Eq.5) the actual global buckling stress can be calculated as follows:

$$\sigma_U / f_y = 1 \quad \text{for} \quad \lambda \le 0.3 \tag{11a}$$

$$\sigma_U / f_y = 1 - 0.63(\lambda - 0.3) \quad \text{for} \quad 0.3 \le \lambda \le 1 \tag{11b}$$

$$\sigma_U / f_y = 1/\left(0.8 + \lambda^2\right) \quad \text{for} \quad \lambda > 1 \tag{11c}$$

This buckling curve is shown in Fig.2. It can be seen that the used buckling curve contains the effect of initial imperfections $(a_0 \ne 0)$ and residual welding stresses $(\sigma_R \ne 0)$, therefore it gives much lower values that the classical critical buckling curve, which neglects these effects.

The global buckling constraint is defined by

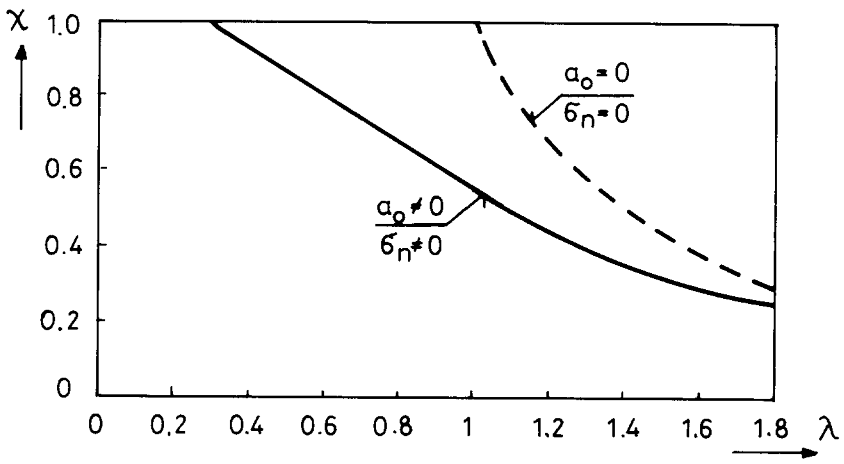

Fig.2. Global buckling curve considering the effect of initial imperfections $(a_0 \neq 0)$ and residual welding stresses $(\sigma_R \neq 0)$

$$\frac{N}{A} \leq \sigma_U^* = \sigma_U \frac{\rho_P}{1+\delta_S} \tag{12}$$

where

$$A = Bt_F + (\varphi - 1)A_S \tag{13}$$

and $$\delta_S = \frac{A_S}{bt_F} \tag{14}$$

ρ_P can be determined considering the single panel buckling of the base plate parts between the stiffeners. The factor $\rho_P / (1+\delta_S)$ expresses the effect of the effective width of the base plate parts.

3.2 Single panel buckling

This constraint eliminates the local buckling of the base plate parts between the stiffeners. From the classical buckling formula for a simply supported uniformly compressed in one direction

$$\sigma_{crP} = \frac{4\pi^2 E}{10.92}\left(\frac{t_F}{b}\right)^2 \tag{15}$$

the reduced slenderness is

$$\lambda_P = \left(\frac{4\pi^2 E}{10.92 f_y} \right)^{1/2} \frac{b}{t_F} = \frac{b/t_F}{56.8\varepsilon} \; ; \qquad \varepsilon = \left(\frac{235}{f_y} \right)^{1/2} \tag{16}$$

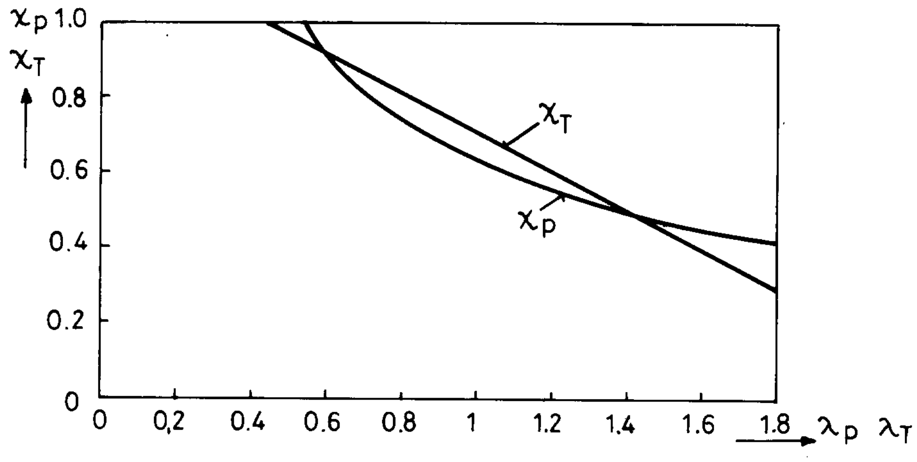

Fig.3. Limiting curves for local plate buckling (χ_P) and torsional buckling of open section ribs (χ_T)

and the actual local buckling stress considering the initial imperfections and residual welding stresses is

$$\sigma_{UP} / f_y = 1 \qquad \text{for} \qquad \lambda_P \le 0.526 \tag{17a}$$

$$\frac{\sigma_{UP}}{f_y} = \left(\frac{0.526}{\lambda_P} \right)^{0.7} \qquad \text{for} \qquad \lambda_P \ge 0.526 \tag{17b}$$

This buckling curve is shown in Fig.3.

Then the factor ρ_P is as follows:

$$\rho_P = 1 \qquad \text{if} \qquad \sigma_{UP} > \sigma_U \tag{18a}$$

$$\rho_P = \sigma_{UP} / f_y \qquad \text{if} \qquad \sigma_{UP} \le \sigma_U \tag{18b}$$

3.3 Local and torsional buckling of stiffeners

These instability phenomena depend on the shape of stiffeners and will be treated separately for flat, L- and trapezoidal stiffeners.

The torsional buckling constraint for open section stiffeners is

$$N / A \le \sigma_{UT} \tag{19}$$

The classical torsional buckling stress is [1]

$$\sigma_{crT} = \frac{GI_T}{I_P} + \frac{EI_\omega}{L^2 I_P} \tag{20}$$

where $G = E/2.6$ is the shear modulus, I_T is the torsional moment of inertia, I_P is the polar moment of inertia and I_ω is the warping constant. The actual torsional buckling stress can be calculated in the function of the reduced slenderness

$$\lambda_T = \left(f_y / \sigma_{crT} \right)^{1/2} \tag{21}$$

$$\sigma_{UT} / f_y = 1 \qquad \text{for} \qquad \lambda_T \le 0.45 \tag{22a}$$

$$\frac{\sigma_{UT}}{f_y} = 1 - 0.53(\lambda_T - 0.45) \qquad \text{for} \qquad 0.3 \le \lambda_T \le 1.41 \tag{22b}$$

$$\frac{\sigma_{UT}}{f_y} = \frac{1}{\lambda_T^2} \qquad \text{for} \qquad \lambda_T \ge 1.41 \tag{22c}$$

This buckling curve is shown in Fig.3.

It should be noted that the interaction of above treated instability phenomena (coupled instability) is not considered here, since it has been shown [1] that this interaction can be neglected when the effect of initial imperfections and residual welding stresses is taken into account for individual buckling modes.

3.4 Distortion constraint

In order to assure the quality of this type of welded structures large deflections due to weld shrinkage should be avoided. It has been shown that the curvature of a beam-like structure due to shrinkage of longitudinal welds can be calculated by relatively simple formulae [9]. The allowable residual deformations f_0 are prescribed by design rules. For compression struts Eurocode 3 (EC3) [13] prescribes $f_0 = L/1000$, thus the distortion constraint is defined as

$$f_{\max} = CL^2 / 8 \le f_0 = L / 1000 \tag{23}$$

where the curvature is for steels

$$C = 0.844x10^{-3} Q_T y_T / I_x \tag{24}$$

Q_T is the heat input, y_T is the weld eccentricity

$$y_T = y_G - t_F / 2 \tag{25}$$

I_x is the moment of inertia of the cross-section containing a stiffener and the base plate strip of width b. The related formulae are given separately for each type of stiffeners.

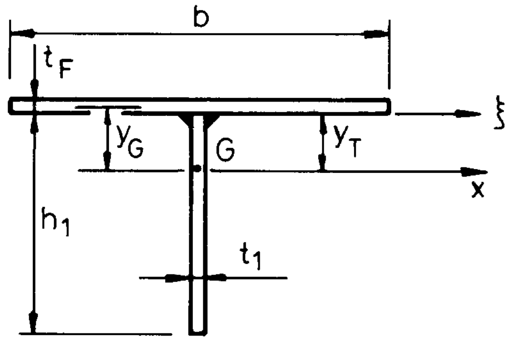

Fig.4. Dimensions of a flat stiffener

4. Formulae for different stiffener shapes

4.1 Flat stiffeners (Fig.4)

$$A_S = h_1 t_1 \ ; \qquad I_S = h_1^3 t_1 / 3 \ ; \qquad y_G = \frac{h_1 + t_F}{2} \frac{\delta_S}{1+\delta_S} \tag{26}$$

$$I_x = \frac{h_1^3 t_1}{12} + h_1 t_1 \left(\frac{h_1}{2} - y_G \right)^2 + \frac{b t_F^3}{12} + b t_F y_G^2 \tag{27}$$

For GMAW-M (Gas Metal Arc Welding with mixed gas) welded fillet welds

$$C_2 a_w^n = 0.3258 x 10^{-3} a_w^2 \qquad (L \text{ in mm}) \tag{28}$$

$a_W = 0.4 t_1$, but $a_{Wmin} = 4$ mm.

When the double fillet welds are welded in such a manner that the second weld is performed after the cooling of the first one

$$Q_T = 1.3 x 59.5 a_w^2 \tag{29}$$

It should be noted that, in the case of simultaneous welding of the two welds, $Q_T = 2.5 x 59.5 a_w^2$, since in this case the plastic zone is much larger than in the previous case.

The local buckling constraint according to EC3 is

$$h_1 / t_1 \le 14\varepsilon \tag{30}$$

In the torsional buckling constraint the following formulae are valid:

$$I_T = h_1 t_1^3 / 3 \ ; \quad I_P = I_S \ ; \qquad I_\omega = 0 \tag{31}$$

4.2 L-stiffeners (Fig.5)

We calculate with cold-formed thin-walled L-section stiffeners of thickness t_2 neglecting the the effect of the rounding of the corner.

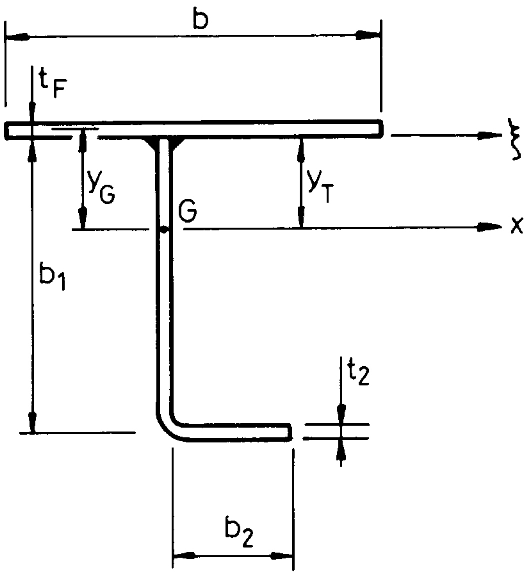

Fig.5. Dimensions of a L-stiffener

$$A_S = (b_1 + b_2)t_2 \ ; \qquad I_S = b_1^3 t_1 / 3 + b_1^2 b_2 t_2 \tag{32}$$

$$y_G = \frac{b_1 t_2 (b_1 + t_F)/2 + b_2 t_2 (b_1 + t_F/2)}{bt_F + A_S} \tag{33}$$

$$I_x = \frac{bt_F^3}{12} + bt_F y_G^2 + \frac{b_1^3 t_2}{12} + b_1 t_2 \left(\frac{b_1}{2} - y_G\right)^2 + b_2 t_2 (b_1 - y_G)^2 \tag{34}$$

$a_W = 0.5t_2$, but $a_{Wmin} = 4$ mm.

Local buckling constraints according to [14] are

$$b_1 / t_2 \le 30\varepsilon \ ; \qquad b_2 / t_2 \le 12.5\varepsilon \tag{35}$$

These constraints can be treated as active.

Furthermore

$$I_T = (b_1 + b_2)t_2^3 / 3 \ ; \qquad I_P = I_S + b_2^3 t_2 / 3 \ ; \qquad I_\omega = b_1^2 b_2^3 t_2 / 3 \tag{36}$$

4.3 Trapezoidal stiffeners (Fig.6)

$$A_S = (a_1 + 2a_2)t_3 \ ; \qquad I_S = a_1 h_3^3 t_3 + \frac{2}{3} a_2^3 t_3 \sin^2 \alpha \tag{37}$$

According to [15] $a_1 = 90$, $a_3 = 300$ mm, thus

$$h_3 = \left(a_2^2 - 105^2\right)^{1/2} \;; \qquad \sin^2\alpha = 1 - \left(\frac{105}{a_2}\right)^2 \tag{38}$$

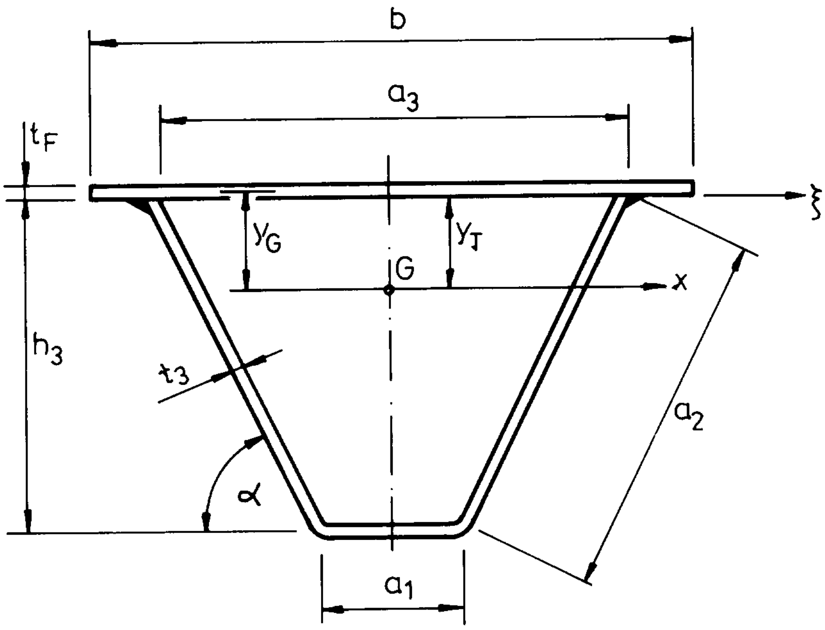

Fig.6. Dimensions of a trapezoidal stiffener

$$y_G = \frac{a_1 t_3 \left(h_3 + t_F / 2\right) + 2a_2 t_3 \left(h_3 + t_F\right)/2}{b t_F + A_S} \tag{39}$$

$$I_x = \frac{b t_F^3}{12} + b t_F y_G^2 + a_1 t_3 \left(h_3 + \frac{t_F}{2} - y_G\right)^2 + \frac{1}{6} a_2^3 t_3 \sin^2\alpha + 2a_2 t_3 \left(\frac{h_3 + t_F}{2} - y_G\right)^2 \tag{40}$$

$a_W = 0.5t_3$, but $a_{Wmin} = 4$ mm.

Local buckling of a trapezoidal stiffener is defined as

$$a_2 / t_3 \le 38\varepsilon \tag{41}$$

This constraint is treated as active.

The single panel buckling constraint is given by Eqs 15-17, but, in the case of trapezoidal stiffeners, instead of b the larger value of $a_3 = 300$ and $b_3 = b - 300$ should be considered. Furthermore, the heat input for a stiffener is

$$Q_T = 2x59.5a_W^2 \tag{42}$$

5. Numerical example

Given data: B = 6000 mm, L = 3000 mm, $N = 1.974 \times 10^7$ [N], f_y = 235 MPa, $E = 2.1 \times 10^5$ MPa, $G = E/2.6$, $\rho = 7.85x10^{-6}$ kg/mm^3, $\Theta_d = 3$.

The variables are as follows: φ, t_F as well as t_1, t_2 and t_3 for flat, L- and trapezoidal stiffeners, respectively. The optima are computed using the Rosenbrock's Hillclimb mathematical programming method complemented by the final search for discrete rounded values [1]. The results are summarized in Tables 1, 2, and 3 as well as in Fig.7. The minimum costs for k_f/k_m = 2 are denoted by bold numbers.

Table 1. Optimum dimensions in mm of compressed plates with flat stiffeners

k_f/k_m (kg/min)	φ	t_F	t_1	K/k_m (kg)
0	10	17	14	2984
1	7	20	14	4142
	4	26	14	5092
2	5	22	14	**4783**
	6	21	14	4930
	7	20	14	5070

Table 2. Optimum dimensions in mm of compressed plates with L-stiffeners

k_f/k_m (kg/min)	φ	t_F	t_2	K/k_m (kg)
0	5	26	10	4074
1	5	26	10	4756
	3	30	10	5386
2	4	27	10	**5266**
	5	26	10	5439
	6	25	10	5601

Table 3. Optimum dimensions in mm of compressed plates with trapezoidal stiffeners

k_f/k_m (kg/min)	φ	t_F	t_3	K/k_m (kg)
0	9	18	10	3344
1	7	20	10	4272
	3	31	10	5538
2	4	25	10	**4956**

5	23	10	4969
6	22	10	5127

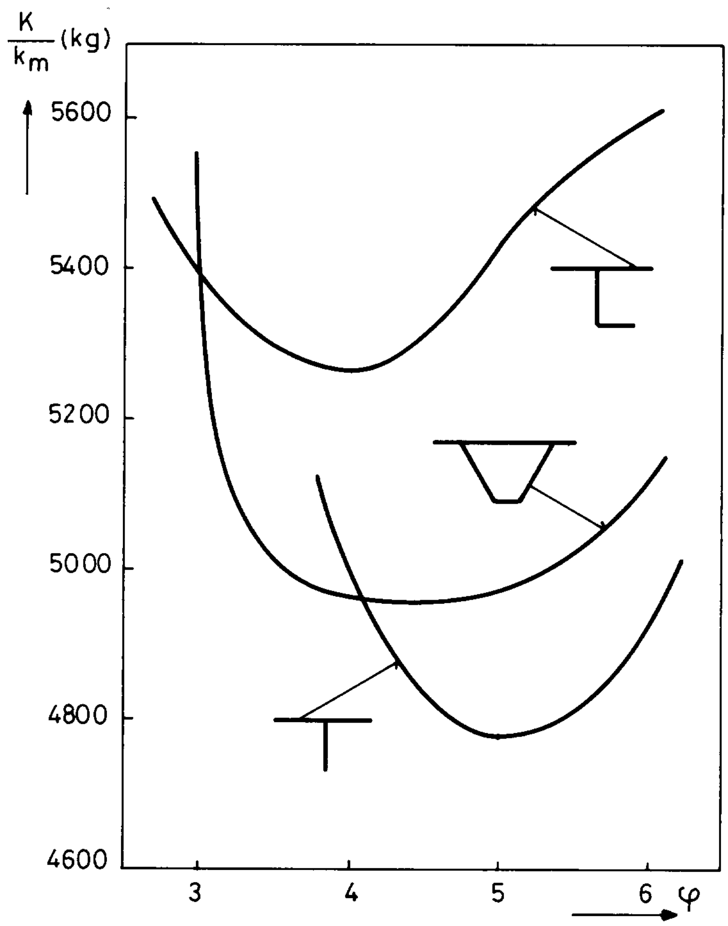

Fig.7. Cost curves in the region of the optimum number of ribs flat, L- and trapezoidal stiffeners

It can be seen that, for this numerical example, the most efficient version is the plate with flat stiffeners. Comparison shows that the trapezoidal and L-stiffeners give costs for k_f/k_m = 2 kg/min (4956-4783)/4783x100 = 3.6% and 10% larger, respectively. This efficiency is caused by the fact that flat stiffeners can be thicker than trapezoidal or L-stiffeners, since the thickness of these ribs is limited by cold-forming requirement.

Fig.7 shows the curves of cost function for k_f/k_m = 2 kg/min for different shapes of ribs. It can be seen that, in the regions of φ illustrated in Fig.7 the cost differences between the best and worst versions are as follows: for flat stiffeners (5092-4783)/4783x100 = 6%, for L-stiffeners 6% and for trapezoidal stiffeners 11%, so it is necessary to optimize the number of stiffeners.

The effect of fabrication cost can be shown comparing the optimum versions for k_f/k_m = 0, 1 and 2. Since the optimum number of stiffeners is low, the fabrication costs are also low compared to the material costs. For instance, in the case of L-stiffeners, the relative cost difference between the versions for k_f/k_m = 0 and 2 kg/min is (5439-4074)/5439x100 = 25%. Thus, the fabrication cost is 25% of the total cost. In spite of this low % the fabrication cost affects the optimum number of stiffeners, since it can be seen that for larger k_f/k_m-value the optimum number of ribs is lower.

Conclusions

Cost comparisons of structural versions obtained for a given numerical example by minimum cost design show the following:

(a) Flat stiffeners give the cheapest version, the cost of plates with L- and trapezoidal ribs is 10% and 3.6% larger, since their thickness is limited.

(b) Since the optimum number of stiffeners is low, the fabrication cost is also low compared to the total cost. In spite of this fact, the fabrication cost affects the optimum number of ribs.

(c) The cost difference between the best and worst solutions in the investigated region of stiffeners' number is significant, which emphasizes the necessity of optimization.

(d) The active constraints are as follows: the global buckling of stiffened plate, the torsional buckling of open-section ribs. The distortion constraint in this case is passive. If the number of stiffeners would be greater, the distortion constraint could be active.

Acknowledgements

This work has been supported by grants OTKA 19003 and OTKA 22846 of the Hungarian Fund of Scientific Research.

References

1. Farkas,J., Jármai,K.: Analysis and optimum design of metal structures. Balkema, Rotterdam-Brookfield, 1997.
2. Farkas,J.,Jármai,K.: Economic design of welded steel structures. J. Constructional Steel Research 46(1998) Nos.1-3. 35-36. Full paper on CD-ROM. Paper No.142.
3. Jármai,K., Horikawa,K., Farkas,J.: Economic design of steel bridge decks with open ribs. Transactions of JWRI (Joining and Welding Research Institute Osaka University) 26(1997)No.1 147-161.

4. Jármai,K.,Farkas,J., Horikawa,K.: Economic design of steel bridge decks. Welding in the World 41(1998)No.1. 49-59.

5. American Petroleum Institute API Bulletin on design of flat plate structures. Bulletin 2V. Washington, 1987.

6. Mikami,I., Niwa,K. Ultimate compressive strength of orthogonally stiffened steel plates. J. Structural Engineering ASCE 122(1996)No.6. 674-682.

7. Discussion of [6] by Bedair,O. and authors' closure. J.Struct.Engng 123(1997)No.8.1116-1119.

8. Jármai,K., Farkas,J.: Cost calculation and optimization of welded steel structures. J. Construct.Steel Res. 50(1999)No.2. 115-135.

9. Farkas,J.,Jármai,K.: Analysis of some methods for reducing beam curvatures due to weld shrinkage. Welding in the World 41(1998)No.4. 385-398.

10. Farkas,J.,Jármai,K.: Optimum design of a stiffened conical roof considering the residual welding distortions. IIW-Doc. XV-986-98. Hamburg, 1998.

11. COSTCOMP Programm zur Berechnung der Schweisskosten. Deutscher Verlag für Schweisstechnik, Düsseldorf, 1990.

12. Bodt,H.J.M.: The global approach to welding costs. The Netherlands Institute of Welding. The Hague, 1990.

13. Eurocode 3. Design of steel structures. Part 1.1. General rules and rules for buildings. European Prestandard ENV 1993-1-1. CEN European Committee for Standardisation, Brussels, 1992.

14. DASt (Deutscher Ausschuss für Stahlbau) Richtlinie 016. Bemessung und konstruktive Gestaltung von Tragwerken aus dünnwandigen kaltgeformten Bauteilen. Köln, 1986.

15. Stahlbau Handbuch Band 2. Köln, Stahlbau-Verlag, 1985.